

Self-similar dynamics of morphogen gradients

Cyrill B. Muratov*, Peter V. Gordon† Stanislav Y. Shvartsman‡

October 19, 2018

Abstract

We discovered a class of self-similar solutions in nonlinear models describing the formation of morphogen gradients, the concentration fields of molecules acting as spatial regulators of cell differentiation in developing tissues. These models account for diffusion and self-induced degradation of locally produced chemical signals. When production starts, the signal concentration is equal to zero throughout the system. We found that in the limit of infinitely large signal production strength the solution of this problem is given by the product of the steady state concentration profile and a function of the diffusion similarity variable. We derived a nonlinear boundary value problem satisfied by this function and used a variational approach to prove that this problem has a unique solution in a natural setting. Using the asymptotic behavior of the solutions established by the analysis, we constructed these solutions numerically by the shooting method. Finally, we demonstrated that the obtained solutions may be easily approximated by simple analytical expressions, thus providing an accurate global characterization of the dynamics in an important class of non-linear models of morphogen gradient formation. Our results illustrate the power of analytical approaches to studying nonlinear models of biophysical processes.

1 Introduction

Reaction-diffusion processes are involved in multiple aspects of embryogenesis. In particular, a combination of extracellular diffusion and degradation of locally produced proteins can establish concentration fields of chemical signals that control spatial and temporal gene expression patterns in developing tissues [1]. Such concentration fields are known as morphogen gradients and have been identified in contexts as diverse as neural development in vertebrates and wing morphogenesis in insects [2, 3].

*Department of Mathematical Sciences, New Jersey Institute of Technology, Newark, NJ 07102, USA

†Department of Mathematical Sciences, New Jersey Institute of Technology, Newark, NJ 07102, USA

‡Department of Chemical Engineering and Lewis Sigler Institute for Integrative Genomics, Princeton University, Princeton, NJ 08544, USA

A canonical model of morphogen gradient formation is given by the following initial boundary value problem [4–8]:

$$\frac{\partial C}{\partial t} = D \frac{\partial^2 C}{\partial x^2} - k(C)C, \quad C(x, t = 0) = 0, \quad (1)$$

$$-D \left. \frac{\partial C}{\partial x} \right|_{x=0} = Q, \quad C(x = \infty, t) = 0. \quad (2)$$

Here $C = C(x, t)$ is the concentration of a morphogen as a function of distance $x \geq 0$ to the tissue boundary and time $t \geq 0$. The morphogen is produced with a constant rate Q at the tissue boundary ($x = 0$), diffuses with diffusivity D in the tissue ($x > 0$) and is degraded in the tissue following some rate law characterized by the pseudo first-order rate constant $k(C) > 0$. This model provides a minimal description of complex biochemical and cellular processes in real tissues, and has been recently used to quantitatively describe morphogen gradients in a number of experimental systems [4, 9–11].

The level of gene expression in a particular cell located a certain distance away from the signal source depends only on the local concentration of that signal (or, more generally, on its time history at that location). Some of the genes controlled by morphogen gradients are directly involved in regulating processes of cell differentiation. Another subset of genes act more indirectly, regulating morphogens themselves. For example, morphogens can control the expression of cell surface molecules that accelerate the rate of morphogen degradation, establishing a feedback loop. Such self-induced morphogen degradation can be modeled by having the degradation constant $k(C)$ to be an increasing function of concentration.

The presence of cooperative effects that are commonly observed in the transcriptional responses to morphogen gradients [3] suggests to consider a general class of degradation rates given by a power law [4]:

$$k(C) = k_n C^{n-1}, \quad n > 1. \quad (3)$$

This type of nonlinearity was first considered by Eldar *et al.*, who demonstrated that power law degradation kinetics may generate morphogen gradients that are robust with respect to large variations in the source strength [4]. They based their conclusions on the analysis of the steady version of Eq. (1). Specifically, they demonstrated that, unlike the solutions of the corresponding linear problem, i.e., Eqs. (1) and (2) with $k(C) \equiv \text{const}$ (in which the solution depends on Q multiplicatively), the stationary solution $C_s(x)$ of Eqs. (1)–(3) approaches an asymptotic limit when $Q \rightarrow \infty$. As a consequence, the steady state of a system operating in the regime of large Q 's will be insensitive to variations in the strength of the source. This has important implications for robustness of steady morphogen gradients established by localized production, diffusion and self-induced degradation.

In this paper we show that robustness of the steady state solutions of Eqs. (1)–(3) discussed above carries over to the solutions of the full time-dependent problem. Remarkably, we found that for large values of Q the solution of the initial boundary value problem given

by Eqs. (1)–(3) approaches a *self-similar* form:

$$C(x, t) = C_s(x)\phi(x/\sqrt{Dt}), \quad (4)$$

where $\phi(\xi)$ is a universal function of $\xi = x/\sqrt{Dt}$ which depends only on n and decreases monotonically from $\phi = 1$ at $\xi = 0$ to $\phi = 0$ at $\xi = \infty$. The self-similar profile function $\phi(\xi)$ is obtained by considering the singular version of the initial boundary value problem with $Q = \infty$.

Our results can be summarized as follows. We derived a nonlinear boundary value problem satisfied by $\phi(\xi)$. We used a variational approach to prove that this problem has a unique solution in a natural setting. Using the asymptotic behavior of the solutions established by the analysis, we constructed these solutions numerically by the shooting method. We also showed that the obtained solutions may be easily fitted to simple analytical expressions, thus providing an accurate global characterization of the dynamics in an important class of non-linear models of morphogen gradient formation. For example, in the biophysically important case $n = 2$, in which the feedback is mediated by the simplest bimolecular interaction our approach yields

$$C(x, t) \approx \frac{6\phi(x/\sqrt{Dt})}{\left(x\sqrt{k_2/D} + (12\sqrt{k_2D}/Q)^{1/3}\right)^2}, \quad (5)$$

$$\phi(\xi) \approx \frac{4000 + \xi^9}{4000 + 5\xi^6 e^{\frac{1}{4}\xi^2}}, \quad n = 2. \quad (6)$$

A comparison of the prediction of Eqs. (5) and (6) with the numerical solution of Eqs. (1)–(3) for a representative set of parameters is presented in Fig. 1.

This paper is organized as follows. We first introduce the non-dimensionalization of the considered initial boundary value problem and give scaling arguments that lead us to consider singular self-similar solutions of the problem. We then undertake a rigorous analysis of existence, uniqueness and qualitative properties of the considered self-similar solutions, which are summarized in Theorem 1. After that, we perform a numerical study of self-similar solutions whose existence was established in the Analysis section and discuss their implications to the dynamics. Finally, we discuss the obtained results in connection with the studies of other types of self-similar solutions in the considered problem, their significance for the threshold crossing and conclude with some open problems.

2 Results

In this section, we formulate a general setting for the analysis of Eqs. (1)–(3) and present our main findings.

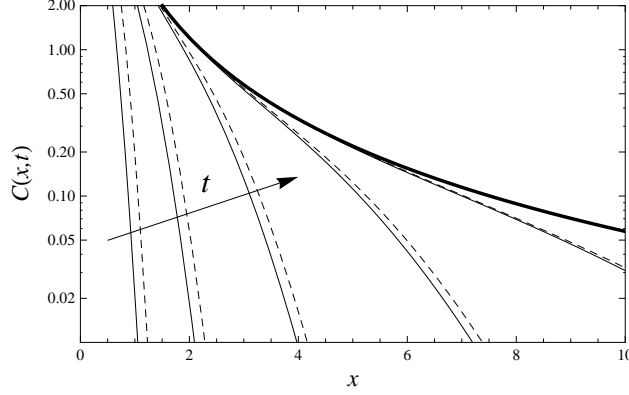


Figure 1: Comparison of the numerical solution of Eqs. (1)–(3) for $n = 2$, $D = 1$, $k_2 = 1$ and $Q = 10^3$ (thin solid lines) with the prediction of Eqs. (5) and (6) (dashed lines) at times $t = 0.04, 0.16, 0.64, 2.56, 10.24$. Thick solid line shows the steady state.

2.1 Non-dimensionalization

We begin by introducing the following dimensionless variables

$$x' = \frac{x}{L}, \quad t' = \frac{t}{T}, \quad u = \frac{C}{C_0}, \quad (7)$$

where

$$L = \left(\frac{D}{k_n C_0^{n-1}} \right)^{1/2}, \quad T = \frac{1}{k_n C_0^{n-1}}, \quad (8)$$

and C_0 is some reference morphogen concentration, corresponding, e.g., to the threshold of expression of a downstream regulated gene. In these new variables, the initial boundary value problem in Eqs. (1)–(3) takes the form

$$\begin{cases} u_t = u_{xx} - u^n & (x, t) \in [0, \infty) \times (0, \infty), \\ u_x(0, t) = -\alpha & t \in (0, \infty), \\ u(x, 0) = 0 & x \in [0, \infty). \end{cases} \quad (9)$$

where

$$\alpha = \frac{Q}{\sqrt{D k_n C_0^{n+1}}} \quad (10)$$

is the dimensionless source strength.

2.2 Scaling arguments

Let us now discuss the approach of the solutions of Eq. (9) to the unique steady state, which for this problem is given explicitly by the following expression [12]:

$$v_\alpha(x) = \left\{ \frac{2(n+1)}{[(2^n(n+1)\alpha^{1-n})^{\frac{1}{n+1}} + (n-1)x]^2} \right\}^{\frac{1}{n-1}}. \quad (11)$$

It is not difficult to see that $u(x, t) \rightarrow v_\alpha(x)$ from below as $t \rightarrow \infty$, implying that the fraction of the steady concentration $u(x, t)/v_\alpha(x)$ reached at a given point $x \geq 0$ at time $t > 0$ will approach unity for $t \gg 1$ [12]. In view of the diffusive nature of the processes involved in establishing the steady concentration profile, one may expect that the approach to the steady state occurs on the scale associated with diffusion. Therefore, to better understand the dynamics, we plot this fraction versus x/\sqrt{t} for the solution of Eq. (9) with $n = 2$ and $\alpha = 1$ obtained numerically for several values of t . The result is presented in Fig. 2. One can see from Fig. 2 that the solution of Eq. (9) at different values of t collapses onto a single master curve for $t \gg 1$. Furthermore, increasing the value of α makes this collapse sooner. We also checked that the same phenomenon occurs for different values of n . This strongly suggests [13] the existence of a hidden self-similarity in the underlying dynamical behavior of the solutions of Eq. (9).

We note that the solutions of Eq. (9) are invariant with respect to the following scaling transformation:

$$\alpha' = \lambda\alpha, \quad t' = \lambda^{\frac{2(1-n)}{1+n}} t, \quad x' = \lambda^{\frac{1-n}{n+1}} x, \quad u' = \lambda^{\frac{2}{n+1}} u. \quad (12)$$

In other words, increasing the source strength α by a factor of λ decreases the time scale of approach to the steady state by a factor of $\lambda^{\frac{2(n-1)}{n+1}}$ at fixed value of x/\sqrt{t} . Therefore, the approach to the universal curve in Fig. 2 must occur on the time scale

$$\tau_n \sim \alpha^{\frac{2(1-n)}{n+1}}. \quad (13)$$

This scale was recently identified by us in the analysis of the local accumulation time in the particular case of Eq. (9) [12]. Observe that $\tau_n \rightarrow 0$ as $\alpha \rightarrow \infty$ for all $n > 1$. Thus, our numerical results suggest that in the limit $\alpha \rightarrow \infty$ the ratio $u(x, t)/v_\alpha(x)$ depends only on x/\sqrt{t} for all $t > 0$, exhibiting self-similar behavior.

2.3 Singular solutions and the similarity ansatz

The numerical observations discussed in the preceding section suggest the need to consider the following singular initial boundary value problem:

$$\begin{cases} u_t = u_{xx} - u^n & (x, t) \in (0, \infty) \times (0, \infty), \\ u(0, t) = \infty, & t \in (0, \infty), \\ u(x, 0) = 0 & x \in (0, \infty). \end{cases} \quad (14)$$

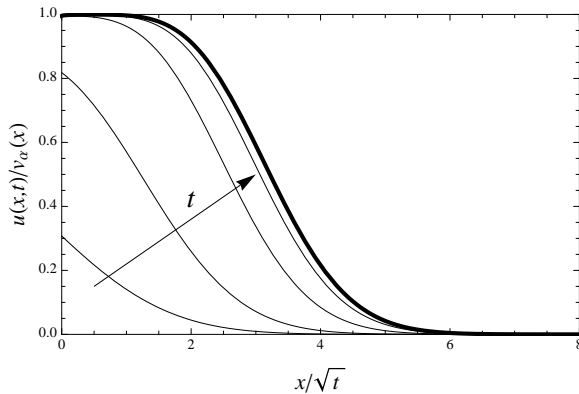


Figure 2: Example of the collapse of the solutions of Eq. (9) onto a universal master curve at large times. Results of the numerical solution of Eq. (9) with $n = 2$ and $\alpha = 1$. Thin lines show snapshots of the solution corresponding to $t = 0.1, 1, 10, 100$ (the direction of time increase is indicated by the arrow). The bold line shows the asymptotic master curve.

By a solution to Eq. (14), we mean a classical solution for all $(x, t) \in (0, \infty) \times (0, \infty)$ decaying sufficiently fast as $x \rightarrow +\infty$ for all $t > 0$, and continuous up to $t = 0$ for all $x > 0$. Note that for each $n > 1$ this problem possesses a *singular* stationary solution

$$v_\infty(x) = \left(\frac{2(n+1)}{(n-1)^2} \right)^{\frac{1}{n-1}} \left(\frac{1}{x} \right)^{\frac{2}{n-1}}, \quad (15)$$

which is the limit of $v_\alpha(x)$ as $\alpha \rightarrow \infty$ for each $x > 0$. Therefore, in view of the discussion above, solution of Eq. (14) is expected to take the form

$$u(x, t) = v_\infty(x)\phi(x/\sqrt{t}), \quad (16)$$

for some universal function $\phi(\xi)$ with values between zero and one, which depends only on n .

We now substitute the similarity ansatz from Eq. (16) into Eq. (14). After some algebra, this leads to the following equation for the self-similar profile ϕ :

$$\xi^2 \frac{d^2 \phi}{d\xi^2} + \left(\frac{\xi^3}{2} - \frac{4\xi}{n-1} \right) \frac{d\phi}{d\xi} + \frac{2(n+1)}{(n-1)^2} \phi(1 - \phi^{n-1}) = 0, \quad (17)$$

which must hold for all $\xi \in (0, \infty)$. Consistent with the interpretation of Eq. (14), this equation needs to be supplemented with the boundary-like conditions

$$\lim_{\xi \rightarrow 0} \phi(\xi) = 1, \quad \lim_{\xi \rightarrow \infty} \phi(\xi) = 0. \quad (18)$$

Existence and multiplicity of solutions of Eqs. (17), (18) are not *a priori* obvious in view of both the non-linearity and the presence of singular terms in the considered boundary value problem. Below we establish existence and uniqueness of these solutions for all $n > 1$ within a natural class of functions. Later, in the following section, we construct these solutions numerically.

2.4 Analysis

This section is concerned with the proof of existence and uniqueness of solutions of Eqs. (17), (18) in a natural setting. The reader interested in the application of our analysis to Eqs. (1)–(3) may skip this part and proceed directly to the following section, which discusses the numerical solution of Eqs. (17), (18).

For the purposes of the analysis it is convenient to rewrite Eq. (17), using a new variable $\zeta = \ln \xi$:

$$\frac{d^2\phi}{d\zeta^2} + \left(\frac{e^{2\zeta}}{2} - \frac{n+3}{n-1} \right) \frac{d\phi}{d\zeta} + \frac{2(n+1)}{(n-1)^2} \phi(1 - \phi^{n-1}) = 0, \quad (19)$$

where $\phi \in C^2(\mathbb{R})$ and has the respective limits

$$\lim_{\zeta \rightarrow -\infty} \phi(\zeta) = 1, \quad \lim_{\zeta \rightarrow +\infty} \phi(\zeta) = 0. \quad (20)$$

We will prove existence and uniqueness of solutions of Eqs. (19) and (20) in the weighted Sobolev space $H^1(\mathbb{R}, d\mu)$, which is obtained as the completion of the family of smooth functions with compact support with respect to the Sobolev norm $\|\cdot\|_{H^1(\mathbb{R}, d\mu)}$, defined as

$$\|w\|_{H^1(\mathbb{R}, d\mu)}^2 = \|w_\zeta\|_{L^2(\mathbb{R}, d\mu)}^2 + \|w\|_{L^2(\mathbb{R}, d\mu)}^2, \quad (21)$$

where $\|w\|_{L^2(\mathbb{R}, d\mu)}^2 = \int_{\mathbb{R}} w^2(\zeta) d\mu(\zeta)$, and the measure $d\mu$ is

$$d\mu(\zeta) = \rho(\zeta) d\zeta, \quad \rho(\zeta) = \exp \left\{ \frac{e^{2\zeta}}{4} - \left(\frac{n+3}{n-1} \right) \zeta \right\}. \quad (22)$$

Our existence and uniqueness result is given by the following theorem.

Theorem 1. *There exists a unique weak solution ϕ of Eq. (19), such that $\phi - \eta \in H^1(\mathbb{R}, d\mu)$, with μ defined in Eq. (22), for every $\eta \in C^\infty(\mathbb{R})$, such that $\eta(\zeta) = 1$ for all $\zeta \leq 0$ and $\eta(\zeta) = 0$ for all $\zeta \geq 1$. Furthermore, $\phi \in C^\infty(\mathbb{R})$, satisfies Eq. (19) classically and $0 < \phi < 1$. In addition, ϕ is strictly decreasing and satisfies Eq. (20).*

Proof. The proof consists of five steps.

Step 1. We first note that Eq. (19) is the Euler-Lagrange equation for the energy functional

$$\mathcal{E}(\phi) = \int_{\mathbb{R}} \left\{ \frac{1}{2} \left(\frac{d\phi}{d\zeta} \right)^2 + \frac{\eta}{n-1} - \frac{\phi^2(n+1 - 2\phi^{n-1})}{(n-1)^2} \right\} d\mu, \quad (23)$$

where $\eta(\zeta)$ is as in the statement of the theorem. The natural admissible class \mathcal{A} for \mathcal{E} is:

$$\mathcal{A} := \{\phi \in H_{\text{loc}}^1(\mathbb{R}) : \phi - \eta \in H^1(\mathbb{R}, d\mu), 0 \leq \phi \leq 1\}. \quad (24)$$

Note that the role of η in the definition of \mathcal{E} is to ensure that the integral in Eq. (23) converges for all $\phi \in \mathcal{A}$. The precise form of $\eta(\zeta)$ is unimportant.

Step 2. We now establish weak sequential lower-semicontinuity and coercivity of the functional \mathcal{E} in the admissible class \mathcal{A} in the following sense: let $\phi_k = \eta + w_k$, where $w_k \rightharpoonup w$ in $H^1(\mathbb{R}, d\mu)$. Then 1) $\liminf_{k \rightarrow \infty} \mathcal{E}(\phi_k) \geq \mathcal{E}(\phi)$, where $\phi = \eta + w$, and 2) if $\mathcal{E}(\phi_k) \leq M$ for some $M \in \mathbb{R}$, then $\|w_k\|_{H^1(\mathbb{R}, d\mu)} \leq M'$ for some $M' > 0$.

Let us introduce the notation $\mathcal{E}(\phi, (a, b))$ for the integral in Eq. (23), in which integration is over all $\zeta \in (a, b)$. Arguing as in [14, Lemma 4.1], for $R \gg 1$ we have

$$\int_R^\infty w^2 d\mu \leq 2e^{-2R} \int_R^\infty w_\zeta^2 d\mu \quad \forall w \in H^1(\mathbb{R}, d\mu). \quad (25)$$

Therefore, from Eq. (25) we find that

$$\mathcal{E}(\phi_k, (R, +\infty)) \geq \left(e^{2R} - \frac{n+1}{(n-1)^2} \right) \int_R^\infty w_k^2 d\mu, \quad (26)$$

which is positive for $R \gg 1$. Similarly, taking into account that the integrand in Eq. (23) is non-negative for $\zeta \leq 0$, we have $\mathcal{E}(\phi_k, (-\infty, 0)) \geq 0$. Since $\mathcal{E}(\cdot, (0, R))$ is lower-semicontinuous by standard theory [15], we obtain $\mathcal{E}(\phi_k) \geq \mathcal{E}(\phi_k, (0, R))$, yielding the first claim in view of arbitrariness of $R \gg 1$.

To prove coercivity, we first note that by Eq. (25)

$$\begin{aligned} \mathcal{E}(\phi_k, (R, +\infty)) &\geq \int_R^\infty \left\{ \frac{1}{2} \left(\frac{dw_k}{d\zeta} \right)^2 - \frac{n+1}{(n-1)^2} w_k^2 \right\} d\mu \\ &\geq \frac{1}{4} \int_R^\infty \left\{ \left(\frac{dw_k}{d\zeta} \right)^2 + w_k^2 \right\} d\mu, \end{aligned} \quad (27)$$

for $R \gg 1$. On the other hand, since $n-1 - \phi^2(n+1 - 2\phi^{n-1}) \geq (n-1)(1-\phi)^2$ for all $0 \leq \phi \leq 1$, we have

$$\mathcal{E}(\phi_k, (-\infty, 0)) \geq \int_{-\infty}^0 \left\{ \frac{1}{2} \left(\frac{dw_k}{d\zeta} \right)^2 + \frac{w_k^2}{n-1} \right\} d\mu. \quad (28)$$

Finally, by boundedness of ϕ_k and η , we also have

$$\mathcal{E}(\phi_k, (0, R)) \geq \frac{1}{4} \int_0^R \left\{ \left(\frac{dw_k}{d\zeta} \right)^2 + w_k^2 \right\} d\mu - CR, \quad (29)$$

for some $C > 0$, whenever $\|w_k\|_{H^1(\mathbb{R}, d\mu)}$ is sufficiently large. So the second claim follows.

Step 3. In view of the lower-semicontinuity and coercivity of \mathcal{E} proved in Step 2, by the direct method of calculus of variations there exists a minimizer $\phi \in \mathcal{A}$ of \mathcal{E} . Noting that $\phi = 0$ and $\phi = 1$ solve Eq. (19), we also have that ϕ is a weak solution of Eq. (19) by continuous differentiability of \mathcal{E} in $H^1(\mathbb{R}, d\mu)$. Furthermore, by standard elliptic regularity theory [16], $\phi \in C^\infty(\mathbb{R})$ and is, in fact, a classical solution of Eq. (19). Also, by strong maximum principle [16], we have $0 < \phi < 1$. To show monotonicity, suppose, to the contrary, that $\phi(a) < \phi(b)$ for some $a < b$. Then $\phi(\zeta)$ attains a local minimum for some $\zeta_0 \in (-\infty, b)$. However, by Eq. (19) we have $d^2\phi(\zeta_0)/d\zeta^2 < 0$, giving a contradiction. By the same argument $d\phi/d\zeta = 0$ is also impossible for any $\zeta \in \mathbb{R}$. Finally, since $\phi - \eta \in H^1(\mathbb{R}, d\mu)$, monotonicity implies Eq. (20).

Step 4. We now discuss the asymptotic behavior of the minimizers obtained in Step 3 as $\zeta \rightarrow +\infty$. Performing the Liouville transformation by introducing $\psi = \phi\sqrt{\rho} \in L^2(R, +\infty)$, where ρ is defined in Eq. (22) and $R \in \mathbb{R}$ is arbitrary, we rewrite Eq. (19) in the form

$$\frac{d^2\psi}{d\zeta^2} = q(\zeta)\psi, \quad \zeta \geq R. \quad (30)$$

Here $q(\zeta) = q_0(\zeta) + q_1(\zeta)$, where

$$q_0(\zeta) = \frac{1}{4} \left(\frac{e^{4\zeta}}{4} + \frac{n-5}{n-1} e^{2\zeta} + 1 \right), \quad (31)$$

$$q_1(\zeta) = \frac{2(n+1)}{(n-1)^2} \phi^{n-1}(\zeta). \quad (32)$$

Observe that $q(\zeta) \geq q_0(\zeta) \geq \frac{1}{4} > 0$ for all $\zeta \geq R \gg 1$. Therefore, Eq. (30) has two linearly-independent positive solutions ψ_1 and ψ_2 , such that $\psi_1 \rightarrow 0$ and $\psi_2 \rightarrow \infty$ together with their derivatives as $\zeta \rightarrow +\infty$ (see e.g. [17]). In particular, $\psi = C\psi_1 \in L^2(R, +\infty)$ for some $C > 0$, and

$$q_1(\zeta) = o(\rho^{\frac{1-n}{2}}), \quad (33)$$

so $q_1(\zeta)$ has a super-exponential decay as $\zeta \rightarrow +\infty$.

Now let ψ_0 be the unique positive solution of Eq. (30) with $q = q_0$ and $\psi_0(R) = 1$ which goes to zero as $\zeta \rightarrow +\infty$. Then we claim that $\psi_1(\zeta)/\psi_0(\zeta) \rightarrow c$ for some $0 < c < \infty$. Indeed, after straightforward algebraic manipulations we have

$$\frac{d}{d\zeta} \ln \left(\frac{\psi_1}{\psi_0} \right) = - \int_\zeta^\infty q_1(s) \frac{\psi_1(s)\psi_0(s)}{\psi_1(\zeta)\psi_0(\zeta)} ds. \quad (34)$$

The result then follows by the decay of ψ_0 and ψ_1 and the estimate in Eq. (33) upon integration of Eq. (34).

Step 5. We now prove uniqueness of the obtained solution, taking advantage of a sort of convexity of \mathcal{E} pointed out in [18]. Suppose, to the contrary, that there are two functions $\phi_1, \phi_2 \in \mathcal{A}$ which solve Eq. (19) weakly. Define $\phi^t = \sqrt{t\phi_2^2 + (1-t)\phi_1^2} \in \mathcal{A}$, since in view of the result of Step 4 we have $m < \phi_1/\phi_2 < M$ for some $M > m > 0$. It is easy to see that the function $E(t) := \mathcal{E}(\phi^t)$ is twice continuously differentiable for all $t \in [0, 1]$. A direct computation yields

$$\begin{aligned} \frac{d^2 E(t)}{dt^2} &= \int_{\mathbb{R}} \left\{ \frac{\phi_1^2 \phi_2^2}{(t\phi_2^2 + (1-t)\phi_1^2)^3} \left(\phi_2 \frac{d\phi_1}{d\zeta} - \phi_1 \frac{d\phi_2}{d\zeta} \right)^2 \right. \\ &\quad \left. + \frac{n+1}{2n-2} (\phi_1^2 - \phi_2^2)^2 (t\phi_2^2 + (1-t)\phi_1^2)^{\frac{n-3}{2}} \right\} d\mu(\zeta). \end{aligned} \quad (35)$$

Therefore, $d^2 E(t)/dt^2 > 0$ for all $t \in [0, 1]$, and so $E(t)$ is strictly convex. However, since the map $t \mapsto \phi^t - \eta$ is of class $C^1([0, 1]; H^1(\mathbb{R}, d\mu))$, this contradicts the fact that $dE(0)/dt = dE(1)/dt = 0$ by the assumption that ϕ_1 and ϕ_2 solve weakly Eq. (19) and hence are critical points of \mathcal{E} . \square

Remark 1. Note that the arguments in Step 4 above imply that the asymptotic behavior of the self-similar profile $\phi(\xi)$ as $\xi \rightarrow \infty$ is the same as that of the decaying solution of Eq. (17) linearized around $\phi = 0$. A similar argument shows that the behavior of $\phi(\xi)$ as $\xi \rightarrow 0$ is the same as that of the corresponding solution of Eq. (17) linearized around $\phi = 1$.

2.5 Numerics

We now construct the self-similar profiles, whose existence and uniqueness was established in Theorem 1, numerically for several values of $n > 1$. We use the shooting method to construct the solutions of Eq. (17), which requires knowledge of the asymptotic behavior of $\phi(\xi)$ near $\xi = 0$ and $\xi = \infty$. To obtain this behavior, we linearize Eq. (17) around the equilibria $\phi = 0$ and $\phi = 1$, which is justified by Remark 1. Denote the corresponding solutions of the linearized equations as ϕ_0 and ϕ_1 , respectively. By a direct computation

$$\begin{aligned} \phi_0(\xi) &= C_1 \xi^{\frac{2}{n-1}} M \left(\frac{1}{n-1}, \frac{1}{2}, -\frac{\xi^2}{4} \right) \\ &\quad + C_2 e^{-\frac{1}{4}\xi^2} \xi^{\frac{2}{n-1}} U \left(\frac{1}{2} + \frac{1}{1-n}, \frac{1}{2}, \frac{\xi^2}{4} \right), \end{aligned} \quad (36)$$

where $M(a, b, z)$ and $U(a, b, z)$ are the confluent hypergeometric functions of the first and second kind, respectively [19]. Using the asymptotic expansions of these functions for large z [19], one can see that $\phi_0(\xi) \rightarrow 0$ as $\xi \rightarrow \infty$, if and only if the constant $C_1 = 0$. Therefore, from the asymptotic expansion of U we have

$$\phi(\xi) \sim e^{-\frac{1}{4}\xi^2} \xi^{\frac{5-n}{n-1}}, \quad \xi \rightarrow \infty. \quad (37)$$

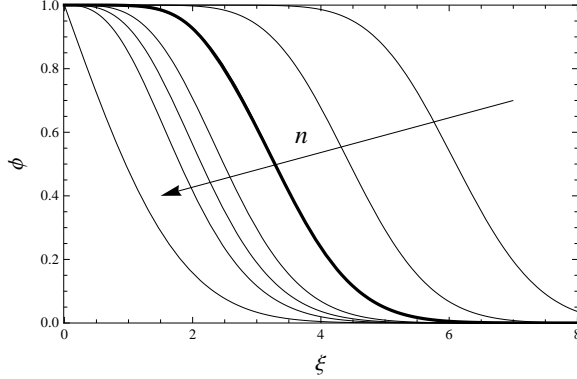


Figure 3: Self-similar profiles $\phi(\xi)$ for different values of n . Results of the numerical solution of Eqs. (17) and (18) for $n = 1.25, 1.5, 2, 3, 4, 6, \infty$. The thick line is the graph of the function given by Eq. (6) overlaying the profile for $n = 2$.

Similarly

$$\phi_1(\xi) = \xi^{\frac{2(n+1)}{n-1}} \left\{ C_1 M \left(\frac{n+1}{n-1}, \frac{5n-1}{2n-2}, -\frac{\xi^2}{4} \right) + C_2 U \left(\frac{n+1}{n-1}, \frac{5n-1}{2n-2}, -\frac{\xi^2}{4} \right) \right\}. \quad (38)$$

Once again, for a bounded solution at $\xi = 0$ we must set $C_2 = 0$, which leads to

$$1 - \phi(\xi) \sim \xi^{\frac{2(n+1)}{n-1}}, \quad \xi \rightarrow 0. \quad (39)$$

The results of the numerical solution of Eq. (17) whose asymptotic behavior is governed by Eqs. (36) and (38) are presented in Fig. 3. One can see that the self-similar profiles form a monotonically decreasing family of functions parametrized by n . The solutions $\phi(\xi)$ approach $\bar{\phi}(\xi) = 1$ on finite intervals as $n \rightarrow 1$ and $\underline{\phi}(\xi) = 1 - \text{erf}(\xi/2)$ as $n \rightarrow \infty$ (the latter solves Eq. (17) corresponding to $n = \infty$). We also found that for the biophysically important case $n = 2$ the self-similar profile can be approximated by the simple expression given by Eq. (6) within $\sim 1\%$ accuracy. The graph of this function, which essentially coincides with that of the numerical solution of Eq. (17) is shown in Fig. 3 with a thick line. Note that this profile also coincides with the limiting profile in Fig. 2 for $t = \infty$.

2.6 Dynamics

We now discuss the dynamical behavior of the obtained self-similar solutions of Eq. (14). The picture remains qualitatively the same for all $n > 1$, so in the following we restrict our attention to the biophysically important case of $n = 2$.

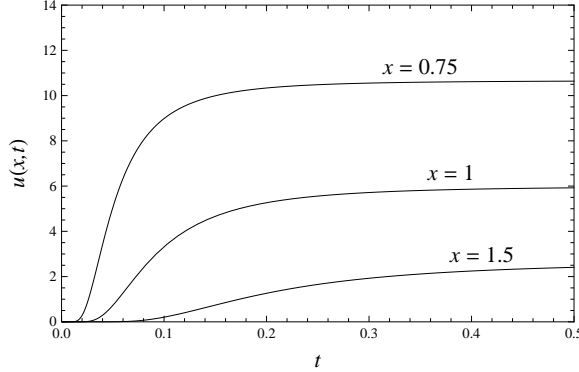


Figure 4: Self-similar solutions $u(x, t)$ of Eq. (14) at several values of x for $n = 2$.

First consider the time course of the solution $u(x, t)$ given by Eq. (16) at a fixed location, i.e. at a fixed value of $x > 0$. From the self-similarity ansatz in Eq. (16) it is clear that the time scale of these dynamics is governed by diffusion, i.e., $t \sim x^2$. A convenient characterization of local dynamical time scale can be made in terms of the local accumulation time $\tau^\infty(x) = \int_0^\infty t p(x, t) dt$, where the probability density-like quantity $p(x, t) = \frac{1}{v_\infty(x)} \frac{\partial u(x, t)}{\partial t}$ [12, 20]. Upon substitution of Eq. (16) into this formula and an integration by parts, one obtains

$$\tau^\infty(x) = ax^2, \quad a = 2 \int_0^\infty \xi^{-3} (1 - \phi(\xi)) d\xi, \quad (40)$$

where numerically $a \simeq 0.122$. We note that by Eq. (39) the integral in Eq. (40) converges for all $n > 1$. The solution for several values of x is shown in Fig. 4. Furthermore, as follows from Eqs. (37) and (39), when $t \ll \tau^\infty(x)$, we have $u(x, t) \sim (x/t^{3/2})e^{-\frac{x^2}{4t}}$, which is exponentially small. At the same time, for $t \gg \tau^\infty(x)$ we have $(v_\infty(x) - u(x, t))/v_\infty(x) \sim (\tau^\infty(x)/t)^3$, i.e., u approaches the stationary solution, with the distance to the stationary solution decaying as $O(t^{-3})$.

We now consider the motion of the level sets of the solutions of Eq. (14). For a given $c > 0$, let us define $x_c(t)$ as the unique value of x , such that $u(x, t) = c$ for each $t > 0$. As follows from Eqs. (16), the function $x_c(t)$ can be determined parametrically as

$$x_c = (6\phi(\xi)/c)^{1/2}, \quad t = 6\phi(\xi)/(c\xi^2), \quad n = 2. \quad (41)$$

The graphs of $x_c(t)$ for a few values of c are shown in Fig. 5. Once again, the dynamics of x_c can be characterized by the local accumulation time $\tau^\infty(x_c^\infty)$ given by Eq. (40), where $x_c^\infty = (6/c)^{1/2}$ is the asymptotic value of $x_c(t)$ as $t \rightarrow \infty$. One can see from Eqs. (37) and (41) that for $t \ll \tau^\infty(x_c^\infty)$ we have $x_c \simeq 2(t \ln t^{-1})^{1/2}$. Thus, all level sets move together for short times, as can also be seen from Fig. 5. On the other hand, for $t \gg \tau^\infty(x_c^\infty)$ the

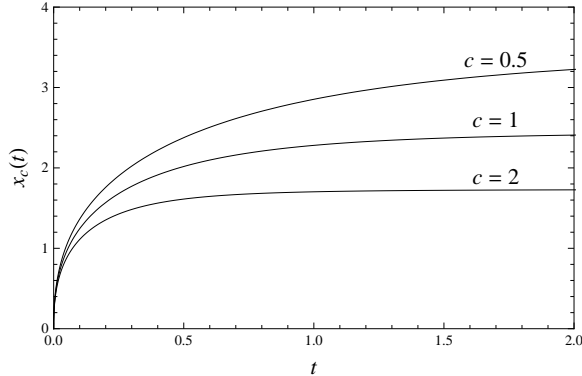


Figure 5: The positions $x_c(t)$ of level sets $\{u(x, t) = c\}$ of the self-similar solution of Eq. (14) at several values of c for $n = 2$.

level set position $x_c(t)$ approaches x_c^∞ as $x_c^\infty - x_c(t) = O(t^{-3})$. Within $\sim 2\%$ accuracy the functions $x_c(t)$ can be approximated by the following simple expression:

$$x_c(t) \approx \left(\frac{4t \ln[3.2 + 6/(ct)]}{1 + 0.76ct} \right)^{1/2}, \quad n = 2. \quad (42)$$

This formula implies that $x_c(t)$ comes within 5% of x_c^∞ at $t \simeq 2\tau^\infty(x_c^\infty)$.

3 Discussion

We have provided an analytical characterization of the dynamics of morphogen concentration profiles in models with self-induced morphogen degradation. Our results reveal the presence of self-similarity in the course of the approach of the concentration profiles to their steady states in either the limit of large source strengths or for large distances away from the source. In addition to demonstrating the self-similar nature of the dynamics, we rigorously established existence and uniqueness of the associated singular self-similar solutions to Eq. (1) and constructed these solutions numerically for several values of n . The obtained solutions may be readily used to study various characteristics of the local kinetics of morphogen concentration. In particular, Eqs. (41) and (42) obtained from the numerical self-similar solutions provide a characterization of threshold crossing events, which determine the times at which a morphogen gradient switches the gene expression on or off at a given point.

3.1 Comparison with self-similar transients

Mathematically, we have constructed a new class of self-similar solutions to Eqs. (1), (3) on half-line. These solutions can be trivially extended to the whole real line by a reflection

and can be viewed as singular solutions of Eqs. (1), (3) that blow up at the origin. We note that Eqs. (1), (3) and their d -dimensional analog is known to possess another kind of self-similar solutions which were extensively studied [21–23], starting from the works of [24, 25] (see also [26] for a less technical introduction and [27] for a variational treatment). These are classical solutions of Eqs. (1), (3) for $t > 0$, which concentrate to a point mass at $t = 0$ and describe the *transient* dynamics for such initial data. They also play an important role in the long-time behavior of the associated initial value problem (see e. g. [24, 28–31]). The solutions found by us can be viewed as the counterparts of the *very singular solutions* constructed in [25]. Our solutions are more singular than those of [25] in the sense that the singularity in the former is concentrated on a half-line ($x = 0, t > 0$) in the (x, t) plane, while the singularity in the latter occurs only at a single point ($x = 0, t = 0$).

3.2 Extensions and open problems

It would be interesting to understand the role our self-similar solutions play for the singular solutions of the initial value problem associated with Eqs. (1), (3) for general non-zero initial data. Let us point out that even the basic questions of existence and uniqueness of such singular solutions for the considered parabolic problems in suitable function classes are currently open (see [32] for a very recent related work). Other natural extensions include higher dimensional versions of the considered problem, as well as a proof of global stability of self-similar solutions. From the point of view of applications, it is also important to consider singular solutions of Eq. (1) for time-varying sources, for which both types of self-similar solutions that are present in the system may be relevant.

Acknowledgements. The work of PVG was supported, in part, by the United States – Israel Binational Science Foundation grant 2006-151. CBM acknowledges partial support by NSF via grants DMS-0718027 and DMS-0908279. SYS acknowledges partial support by NSF via grant DMS-0718604 and by NIH via grant GM078079. CBM and PVG would like to acknowledge valuable discussions with V. Moroz.

References

- [1] A. Martinez-Arias and A. Stewart. *Molecular principles of animal development*. Oxford University Press, New York, 2002.
- [2] T. Tabata and Y. Takei. Morphogens, their identification and regulation. *Development*, 131:703–712, 2004.
- [3] H. L. Ashe and J. Briscoe. The interpretation of morphogen gradients. *Development*, 133:385–394, 2006.

- [4] A. Eldar, D. Rosin, B. Z. Shilo, and N. Barkai. Self-enhanced ligand degradation underlies robustness of morphogen gradients. *Devel. Cell*, 5:635–646, 2003.
- [5] F. Tostevin, P. R. ten Wolde, and M. Howard. Fundamental limits to position determination by concentration gradients. *PLoS Comput. Biol.*, 3:e78, 04 2007.
- [6] H. G. Othmer, K. Painter, D. Umulis, and C. Xue. The intersection of theory and application in elucidating pattern formation in developmental biology. *Math. Model. Nat. Phenom.*, 4:3–82, 2009.
- [7] A. D. Lander, W. C. Lo, Q. Nie, and F. Y. Wan. The measure of success: constraints, objectives, and tradeoffs in morphogen-mediated patterning. *Cold Spring Harbor Perspectives in Biology*, 1:a002022, 2009.
- [8] O. Wartlick, A. Kicheva, and M. Gonzalez-Gaitan. Morphogen gradient formation. *Cold Spring Harbor Perspectives in Biology*, 1(3):a001255, 2009.
- [9] F. He, T. E. Saunders, Y. Wen, D. Cheung, R. Jiao, P. R. ten Wolde, M. Howard, and J. Ma. Shaping a morphogen gradient for positional precision. *Biophys. J.*, 99:697–707, 2010.
- [10] A. Kicheva, P. Pantazis, T. Bollenbach, Y. Kalaidzidis, T. Bittig, F. Julicher, and M. Gonzalez-Gaitan. Kinetics of morphogen gradient formation. *Science*, 315:521–525, 2007.
- [11] S. R. Yu, M. Burkhardt, M. Nowak, J. Ries, Z. Petrasek, S. Scholpp, P. Schwill, and M. Brand. Fgf8 morphogen gradient forms by a source-sink mechanism with freely diffusing molecules. *Nature*, 461:533–536, 2009.
- [12] P. V. Gordon, C. Sample, A. M. Berezhevskii, C. B. Muratov, and S. Y. Shvartsman. Local kinetics of morphogen gradients. *Proc. Natl. Acad. Sci. US.*, 108:6157–6162, 2011.
- [13] G. I. Barenblatt. *Scaling, self-similarity, and intermediate asymptotics*. Cambridge University Press, 1996.
- [14] M. Lucia, C. B. Muratov, and M. Novaga. Linear vs. nonlinear selection for the propagation speed of the solutions of scalar reaction-diffusion equations invading an unstable equilibrium. *Commun. Pure Appl. Math.*, 57:616–636, 2004.
- [15] G. Dal Maso. *An Introduction to Γ -Convergence*. Birkhäuser, Boston, 1993.
- [16] D. Gilbarg and N. S. Trudinger. *Elliptic Partial Differential Equations of Second Order*. Springer-Verlag, Berlin, 1983.

- [17] Giovanni Sansone. *Equazioni Differenziali nel Campo Reale, Vol. 2*. Nicola Zanichelli, Bologna, 1949. 2d ed.
- [18] B. Kawohl. When are solutions to nonlinear elliptic boundary value problems convex? *Comm. Partial Differential Equations*, 10:1213–1225, 1985.
- [19] M. Abramowitz and I. Stegun, editors. *Handbook of mathematical functions*. National Bureau of Standards, 1964.
- [20] A. M. Berezhkovskii, C. Sample, and S. Y. Shvartsman. How long does it take to establish a morphogen gradient. *Biophys. J.*, 99:L59–L61, 2010.
- [21] H. Brézis and A. Friedman. Nonlinear parabolic equations involving measures as initial conditions. *J. Math. Pures Appl.*, 62:73–97, 1983.
- [22] S. Kamin and L. A. Peletier. Singular solutions of the heat equation with absorption. *Proc. Amer. Math. Soc.*, 95:205–210, 1985.
- [23] L. Oswald. Isolated positive singularities for a nonlinear heat equation. *Houston J. Math.*, 14:543–572, 1988.
- [24] V. A. Galaktionov, S. P. Kurdyumov, and A. A. Samarskiĭ. Asymptotic “eigenfunctions” of the Cauchy problem for a nonlinear parabolic equation. *Mat. Sb. (N.S.)*, 126:435–472, 1985.
- [25] H. Brezis, L. A. Peletier, and D. Terman. A very singular solution of the heat equation with absorption. *Arch. Rational Mech. Anal.*, 95:185–209, 1986.
- [26] A. J. Bernoff and T. P. Witelski. Stability and dynamics of self-similarity in evolution equations. *J. Engrg. Math.*, 66:11–31, 2010.
- [27] M. Escobedo and O. Kavian. Variational problems related to self-similar solutions of the heat equation. *Nonlinear Anal.*, 11:1103–1133, 1987.
- [28] M. Escobedo, O. Kavian, and H. Matano. Large time behavior of solutions of a dissipative semilinear heat equation. *Comm. Partial Differential Equations*, 20:1427–1452, 1995.
- [29] J. Bricmont and A. Kupiainen. Stable non-Gaussian diffusive profiles. *Nonlinear Anal.*, 26:583–593, 1996.
- [30] C. E. Wayne. Invariant manifolds for parabolic partial differential equations on unbounded domains. *Arch. Rational Mech. Anal.*, 138:279–306, 1997.
- [31] L. Herraiiz. Asymptotic behaviour of solutions of some semilinear parabolic problems. *Ann. Inst. H. Poincaré Anal. Non Linéaire*, 16:49–105, 1999.

- [32] L. Veron. A note on maximal solutions of nonlinear parabolic equations with absorption. arXiv:0906.0669v2 [math.AP], 2011.